

SUPPLEMENTARY INFORMATION

Nanofluidic direct formic acid fuel cell with combined flow-through and air-breathing electrode for high performance

E. Ortiz-Ortega,^a Marc-Antoni Goulet,^b Jin Wook Lee,^c M. Guerra-Balcázar,^a N. Arjona,^d Erik Kjeang,^b J. Ledesma-García,^a and L. G. Arriaga^{‡d}

S1. Fabrication of the Nanofluidic fuel cell.

The fabrication procedure used for our cells consists of only two simple steps. The first step consists of manufacturing the supporting plates using a CNC machining with the top plate including two inlets and a window for gas access (Fig. S1-b) and a bottom plate with one outlet for the reaction by-products. Both plates were made using Poly-(methyl methacrylate) PMMA. The second step consists in patterning a home-made silicone elastomer film (Silastic®, Dow Corning, prepared using an Elcometer® Film Applicator with a final thickness of 200 μm) and cut using a Silhouette® cutting plotter (Fig. S1-b and S1-c, green film). The patterned polymer film compressed between the plates serves as both gasketing and cell channel structure. Electrodes were cut (Fig. S1-d) from commercial carbon nanofoam (Marketech Inc.) and the electrocatalysts were incorporated by spray coating. The air-breathing window was made also using the CNC with a final dimension of 0.22 cm^2 (Fig. S1-d). Pd/C and Pt/C (20 and 30%, respectively, ETEK) catalysts deposition on the carbon nanofoam was made by the spray technique. Briefly, an ink was prepared with 120 μL of isopropyl alcohol per milligram of catalyst and sonicated by 30 minutes. After that, 14 μL of Nafion (5%, diluted in isopropyl alcohol, Electrochem®) per milligram of catalyst was added to the solution and newly sonicated by 30 minutes.

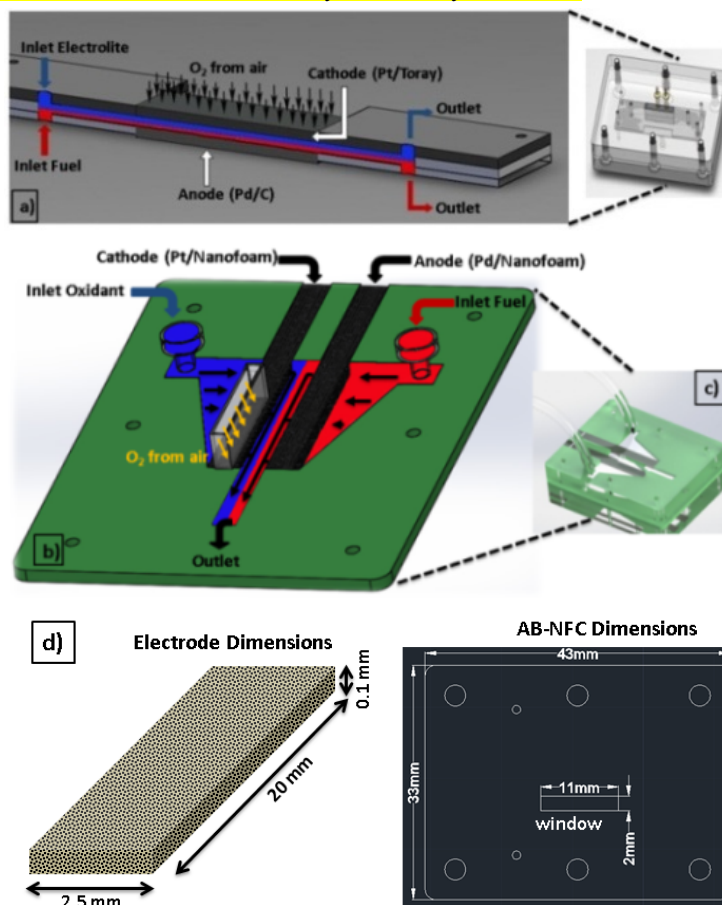


Figure S1. Scheme of a) a classic flow-over air breathing microfluidic fuel cell, b) flow-through air breathing nanofluidic fuel cell, c) assembled AB-NFC and d) three-dimensional nanoporous electrode and air window dimensions

S2. Performance comparison between close and open systems

The formation of a co-laminar interface between the anodic and cathodic streams was verified at $200 \mu\text{L min}^{-1}$ for both fluids; with methylene blue was added as



Figure S2. Top view photograph of the nanofluidic fuel cell. Methylene blue was used as colorant at $200 \mu\text{L min}^{-1}$ flow rate

The air-breathing nanofluidic fuel cell (AB-NFC) exhibited sensitivity to the cathodic flow rate as shown in Figure 2b. For the same purpose, the cell performance was evaluated in a “closed system (no window incorporated in the cell)” and in an “open system (air breathing)” (Fig. S3-a & S3-b, respectively) in order to determine the contribution of oxygen from air and from dissolved oxygen (Fig. S4). The system was closed or opened using two different Poly-(methyl methacrylate) PMMA plates and a Pd effective mass load of 0.3 mg with a flow rate of $200 \mu\text{L min}^{-1}$ for the anodic and the cathodic stream.

The closed system resulted in a power density of 52 mW cm^{-2} ; meanwhile the open system resulted in 70 mW cm^{-2} . The current density was enhanced from 188 mA cm^{-2} to 320 mA cm^{-2} , which is 1.7-fold higher for the air-breathing design. The enhancement of the current density and the power density was expected due to the higher concentration of oxygen and diffusivity in air than in aqueous solution.¹

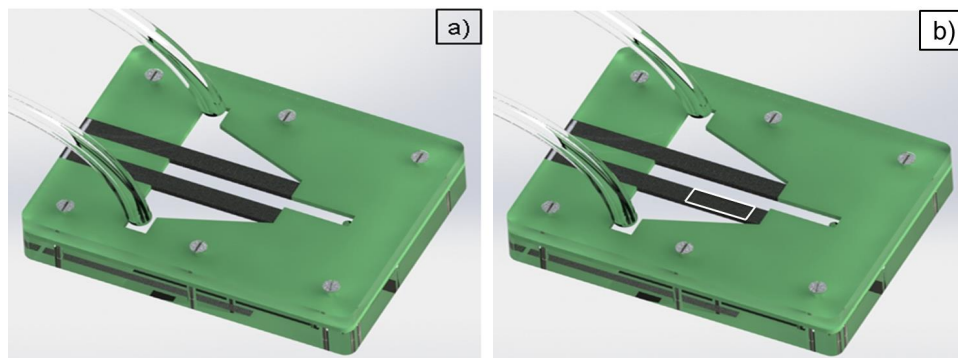


Figure S3. Schematic representation of a) closed and b) open nanofluidic fuel cell.

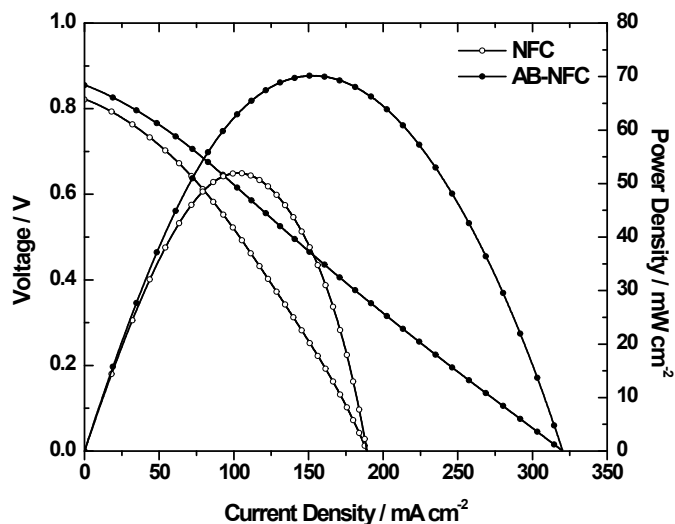


Figure S4. Polarization and power density curves of open (NFC) and closed (AB-NFC) nanofluidic fuel cells using 0.5 M formic acid as fuel.

S3. Stability of the air breathing nanofluidic fuel cell

The stability of the AB-NFC was tested during 120 minutes (Fig. S5) applying two potentials: the potential of maximum current density (0.01 V, top behavior) and the potential of maximum power density (0.42 V, bottom behavior). The cell showed good stability as can be observed with the potential of maximum power density, where the current density decreased from 68 to 56 mA cm⁻² after two hours of continuous operation. It is known that the formic acid electrooxidation reaction can be carried out by a direct oxidation forming CO₂ bubbles or by a secondary pathway which involves the formation and adsorption of CO as a reaction intermediate.² The current density diminished can be attributed to the formation of CO₂ bubbles and the CO adsorption which could poison the electrode surface and lead to reduced active surface area.

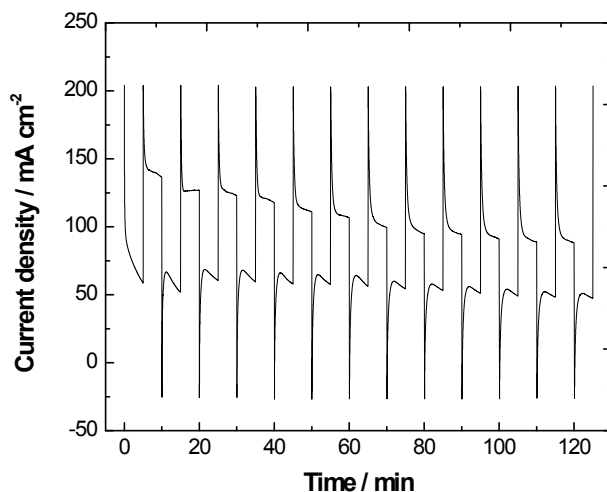


Figure S5. Stability curve at 0.42 and 0.01 V for 0.5 M formic acid in an AB-NFC

S4. State-of-the-art co-laminar flow cells

Table S1 shows a comparison of power density between air-breathing membraneless formic acid fuel cells reported in the literature and the present nanofluidic fuel cell device. Even the power density obtained by the closed nanofluidic fuel cell is comparable with those using oxygen from the air, thus demonstrating the effectiveness of nanofluidic electrode configuration.

Table S1. Comparison of current density and power density values for air-breathing formic acid microfluidic fuel cells reported in the literature.

Fuel / M	OCV/ V	Anode catalyst loading / mg cm ⁻²	Current density / mA cm ⁻²	Power density / mW cm ⁻²	Reference
FA / 1	0.9	10	130	26	1
FA / 0.5	0.85	5	118.3	21.5	3
FA / 3	0.75	7-8	140	29	4
FA / 1	0.95	7-8	120	26.5	5
FA / 1	0.8	10	260	36	6
FA / 1	0.85	10	320	55	6
FA / 1	0.94	10	130	26	7
FA/0.5	0.85	1.2	500	100	This work
FA/0.5	0.82*	0.6	188*	52*	This work

* Indicates the values for closed nanofluidic fuel cell.

References

- (1) Jayashree, R. S.; Gancs, L.; Choban, E. R.; Primak, A.; Natarajan, D.; Markoski, L. J.; Kenis, P. J. A. *J. Am. Chem. Soc.* **2005**, *127*, 16758.
- (2) Yu, X.; Pickup, P. G. *J. Power Sources* **2008**, *182*, 124.
- (3) Zhu, X.; Zhang, B.; Ye, D.-D.; Li, J.; Liao, Q. *J. Power Sources* **2014**, *247*, 346.
- (4) Shaegh, S. A. M.; Nguyen, N.-T.; Chan, S. H. *J. Power Sources* **2012**, *209*, 312.
- (5) Shaegh, S. A. M.; Nguyen, N.-T.; Chan, S. H. *Int. J. Hydrogen Energy* **2012**, *37*, 3466.
- (6) Jayashree, R. S.; Yoon, S. K.; Brushett, F. R.; Lopez-Montesinos, P. O.; Natarajan, D.; Markoski, L. J.; Kenis, P. J. A. *J. Power Sources* **2010**, *195*, 3569.
- (7) Brushett, F. R.; Jayashree, R. S.; Zhou, W.; Kenis, P. J. A. *Electrochim. Acta* **2009**, *54*, 7099.